International Journal of Bifurcation and Chaos, Vol. 33, No. 1 (2023) 2350005 (13 pages)

DOI: 10.1142/S0218127423500050

Exact Solution of Four-Coupled Nonidentical Kuramoto Oscillators at a Full Phase Locked State

M. S. Mahmoud* and M. Medhat†
Department of Physics, Faculty of Science,
Ain Shams University, Abassia, Cairo 11566, Egypt
**mohamedshehata@sci.asu.edu.eg*
†*mmedhat61@sci.asu.edu.eg*

Hilda A. Cerdeira
Instituto de Fisica Teorica,
Sao Paulo State University (UNESP),
Rua Dr. Bento Teobaldo Ferraz 271, Bloco II,
Barra Funda, 01140-070 Sao Paulo, Brazil
hilda.cerdeira@unesp.br

Hassan F. El-Nashar‡
Department of Physics, Faculty of Science,
Ain Shams University, Abassia, Cairo 11566, Egypt
hfelnashar@sci.asu.edu.eg

Received May 21, 2022; Revised October 31, 2022

We consider a Kuramoto model of four-coupled oscillators of nonidentical initial frequencies. Under the influence of coupling, the oscillators fall into a full phase locked state of a common frequency when the coupling strength surpasses a threshold value. We find numerically the parameters that control this distinguishable coupling constant at the moment the oscillators transit into an entire frequency synchronization when a complete phase lock state takes place. We are able to set apart a recognizable phase condition at the fully locked state. This phase condition helps to derive an analytic formula to calculate the coupling factor as soon as the oscillators depart to a full phase locking state. The explicit expression of the edge coupling factor is given in terms of the initial frequencies of the four oscillators. The formula valid for calculating the distinct coupling allows to find mathematical expressions to calculate the phase differences when the four-coupled phase oscillators are strictly at the full phase locked state and have a common frequency synchronization.

Keywords: Frequency synchronization; Kuramoto model; coupled phase oscillators.

1. Introduction

The dynamics of many systems, which appear in physics, chemistry, biology, engineering, technology, social relations, etc., are modeled by coupled oscillators [Strogatz, 2018; Csaba & Porod, 2020; Thiem *et al.*, 2020]. Although the mechanisms of dynamics in the above-mentioned scientific fields are dissimilar, they can successfully, under an assumption of weak coupling, be described by using the Kuramoto model of all-to-all coupled phase oscillators [Guo *et al.*, 2021; Velasco & Neto, 2021; Chheba *et al.*, 2020; Latifpour & Miri, 2020; Heggli *et al.*, 2019;

‡Author for correspondence

Jang *et al.*, 2019; Witthaut *et al.*, 2017]. An interesting feature that is common in the formerly stated systems is synchronization [Wiesenfeld, 2020; Wu & Li, 2020; Yang & Liu, 2020; Young-Pil & Zhuchun, 2019; Boccaletti *et al.*, 2018; Taheri *et al.*, 2017], where the coupled phase oscillators possess a common frequency under the impact of coupling. The synchronous feature of oscillators at a full phase locked state takes place once the coupling factor exceeds a significant threshold value. It is essential to examine the coupled phase oscillators to understand the transition to the full phase locking.

A system of three-coupled phase oscillators is analyzed in [Maistrenko *et al.*, 2004], which was later solved analytically [El-Nashar, 2016, 2017] at a phase lock state. In particular, once the complete frequency synchronization is achieved, it is possible to find an analytic expression of the marked coupling constant, at the phase locked state, and consequently the phase differences in terms of the initial frequencies of the oscillators. In addition, knowing the formula of this distinct coupling value and phase differences, in case of three oscillators, allows to understand quantitatively the mechanism that leads to synchronization and how the oscillators are phase locked at a saddle-node bifurcation [El-Nashar, 2017]. However, in the case of three-coupled phase oscillators, the local and global coupling are the same, while in the systems of a few coupled phase oscillators larger than three, the difference between the locally and globally coupled cases will appear. Systems of a few coupled phase oscillators have been attracting attention from a fundamental and a practical point of view in numerous fields, where synchronization emerges [Huang & Zadeh, 2020; Gourary & Rusakov, 2020; Scholes, 2020; Yap *et al.*, 2019]. The stability of the full phase locked state [Aeyels & Rogge, 2004; Mirollo & Strogatz, 2005], in the case of a finite number of coupled phase oscillators, shows the existence of a stable full phase lock solution when the coupling passes a certain specific value. Therefore, the answer to the issues, *how to distinguish the full phase lock solution* and *what is the explicit formula valid to calculate the coupling strength at the phase locking and hence the phase differences*, will provide further steps towards the understanding of the dynamics of the coupled phase oscillators. Thus, this goal can be achieved when we perform a detailed study considering synchronization at a phase locking state of a few all-to-all coupled phase oscillators starting from four globally coupled phase oscillators.

A system of four all-to-all coupled phase oscillators was examined in [Maistrenko *et al.*, 2005], where the synchronization mechanism was investigated. However, there are no exact analytic solution at the full phase locking, for a system of four-coupled Kuramoto oscillators, neither to present an expression for calculating the coupling factor nor to account for the phase differences at the full phase locked state. Understanding the synchronization of the four Kuramoto oscillators may introduce additional realization of the synchronization mechanisms in systems of a few and a finite number of coupled phase oscillators, which will have remarkable results. The Kuramoto model, for four oscillators is defined as [Strogatz, 2018]

$$\dot{\theta}_j = \omega_j + \frac{K}{4} \sum_{j=1, i \neq j}^{4} \sin(\theta_i - \theta_j), \tag{1}$$

where K is the coupling constant, ω_j and θ_j represent the phase and initial frequency, respectively, for an oscillator and $\dot{\theta}_j$ acts for the time evolution of the phase. As the coupling strength K increases, the oscillators remain desynchronized. When K reaches a critical coupling K_c the oscillators begin to synchronize and hence K_c marks the onset of partial locking and once K finally attains K_c^*, the full phase locking is developed [Aeyels & Rogge, 2004; Mirollo & Strogatz, 2005]. In order to understand quantitatively the transition into a stable phase locking state, the determination of the marked threshold coupling parameters, K_c and K_c^*, is crucial. According to system (1), when the initial frequencies are nonidentical (the oscillators have unequal initial frequencies prior to coupling), a complete frequency synchronization to a common frequency ω_o starts to exist at a value of the coupling constant K_c^*, when a certain stable phase lock state appears, where $\omega_o = (1/4)\sum_{j=1}^{4} \omega_j$. The explicit formula for the coupling constant K_c^* is not known. As clearly seen in Eq. (1), the coupling term, that affects the time evolution of the phase of each oscillator, depends on K as well as the phase differences. The determination of an explicit expression for the coupling constant, for a general set of the initial frequencies $\{\omega_i\}$ that satisfies $(1/4)\sum_{j=1}^{4} \omega_j = \omega_o$, at the transition to the entire phase locked state will help to comprehend the mechanism of the phase dynamics and hence will explain how the oscillators

fall into synchronization when the coupling reaches the effective coupling K_c^*. Also, the determination of an explicit formula for K_c^* will offer not only a framework to understand the feature of the oscillator's synchronization just below K_c^* but also provides the basis to determine the coupling strength K_c. Therefore, the examination of the Kuramoto model of all-to-all four coupled phase oscillators will help to promote additional understanding of the intrinsic dynamics of a few globally coupled phase oscillators. Thus, understanding the synchronization phenomena in a few all-to-all coupled phase oscillators will explore the processes that lead to synchronization in a Kuramoto model of a finite number of oscillators.

In this work, we study four globally coupled phase oscillators of unequal initial frequencies at the transition to synchronization at full phase locking. We start analyzing numerically the frequency synchronization of the four-coupled phase oscillators. Numerical solutions of system (1) are necessary because it allows determining the important parameters that control the effective coupling value at a total phase locked state by finding an approximate expression for the efficient coupling value K_c^*. Also, the numerical investigations guide us to search for the stable phase lock [Aeyels & Rogge, 2004; Mirollo & Strogatz, 2005] situations at the complete phase locking solution. We find the phase lock condition, which enables us to derive an explicit expression for computing the coupling factor K_c^*. The expression for the marked coupling strength K_c^* shows that it depends on the initial frequencies of the individual oscillators. In addition, we are able to obtain formulas for calculating the phase differences at the appearance of the synchronization at the total phase locking state.

This work is organized as follows: In Sec. 2, we demonstrate the synchronization trees for different configurations of the four-coupled oscillators. In Sec. 3, we present a numerical approach to find the most effective parameters (depending on initial frequencies) that decide mainly the values of K_c^*. This numerical work allows to obtain an approximate expression to compute the values of the critical coupling K_c^*. Also, we are able to specify the phase lock condition at the moment the oscillators synchronize in a stable state of full phase locking. In view of the results as per the numerical approach (Sec. 3), in Sec. 4, we present a method to obtain an explicit mathematical expression for the critical coupling constant. In Sec. 5, we find formulas for calculating the phase differences at the stage of synchronization at a full phase locked state. In Sec. 6, a discussion is presented. In Sec. 7, a conclusion is given.

2. Frequency Synchronization Trees

We write the initial frequencies ω_j, $j = 1, 2, 3, 4$, for four oscillators, as $\omega_{\max} > \omega_{m>} > \omega_{m<} > \omega_{\min}$, where we use the condition $(\omega_{\max} + \omega_{m>} + \omega_{m<} + \omega_{\min}) = 0$ which does not change the general feature of the original system (1). We define the maximum frequency detuning quantity $\Delta_{\max} = (\omega_{\max} - \omega_{\min})$, where $\Delta_{\max} > 0$. We also define the frequency difference between the two middle oscillators $\Delta_m = (\omega_{m<} - \omega_{m>})$, where $-\Delta_{\max} \leq \Delta_m \leq 0$. We also define the other two frequency differences $\Delta_u = (\omega_{m>} - \omega_{\max})$ and $\Delta_d = (\omega_{\min} - \omega_{m<})$, where $\Delta_u \leq 0$ and $\Delta_d \leq 0$.

System (1) has several patterns, that show the routes from desynchronization to synchronization, according to the values of the initial frequencies $\omega_{\max}$, $\omega_{m>}$, $\omega_{m<}$ and $\omega_{\min}$. In Fig. 1, we plot the quantities $\langle \dot{\theta}_i \rangle$ versus K, where we show the critical coupling K_c that indicates the onset of partial locking. There are six different patterns in Fig. 1, where the four different quantities $\langle \dot{\theta}_{\max} \rangle \simeq \langle \dot{\theta}_{m>} \rangle \simeq \langle \dot{\theta}_{m<} \rangle \simeq \langle \dot{\theta}_{\min} \rangle$. We indicate, in the legends of all graphs of Fig. 1, the conditions for each pattern. Figure 1(a) shows in the main plot the three oscillators of initial frequencies $\omega_{\max}$, $\omega_{m>}$ and $\omega_{m<}$ meeting oscillator of an initial frequency $\omega_{\min}$ at K_c while in the inset of Fig. 1(a), we depict the case of one oscillators of an initial frequency $\omega_{\max}$ that synchronizes to the three oscillator of $\omega_{m>}$, $\omega_{m<}$ and $\omega_{\min}$. In Fig. 1(b), we introduce in the main graph a case when three oscillators of $\omega_{\max} = \omega_{m>} = \omega_{m<}$ synchronize to the fourth oscillator of $\omega_{\min}$, where $\omega_{\min} = -3\omega_{\max}$. In the inset of Fig. 1(b), we demonstrate the synchronization of the four oscillators that have $\omega_{\max}$ and $\omega_{m>} = \omega_{m<} = \omega_{\min}$, where $\omega_{\max} = -3\omega_{\min}$. The main plot of Fig. 1(c) demonstrates the synchronization of two oscillators coming from above ($\omega_{\max}$ and $\omega_{m>}$ of a larger separation) to meet the other two oscillators which are approaching from below ($\omega_{m<}$ and $\omega_{\min}$ of a smaller separation). The inset of Fig. 1(c) presents a synchronization of two oscillators that are coming from above ($\omega_{\max}$ and $\omega_{m>}$ of a smaller separation) to meet the other two oscillators which are

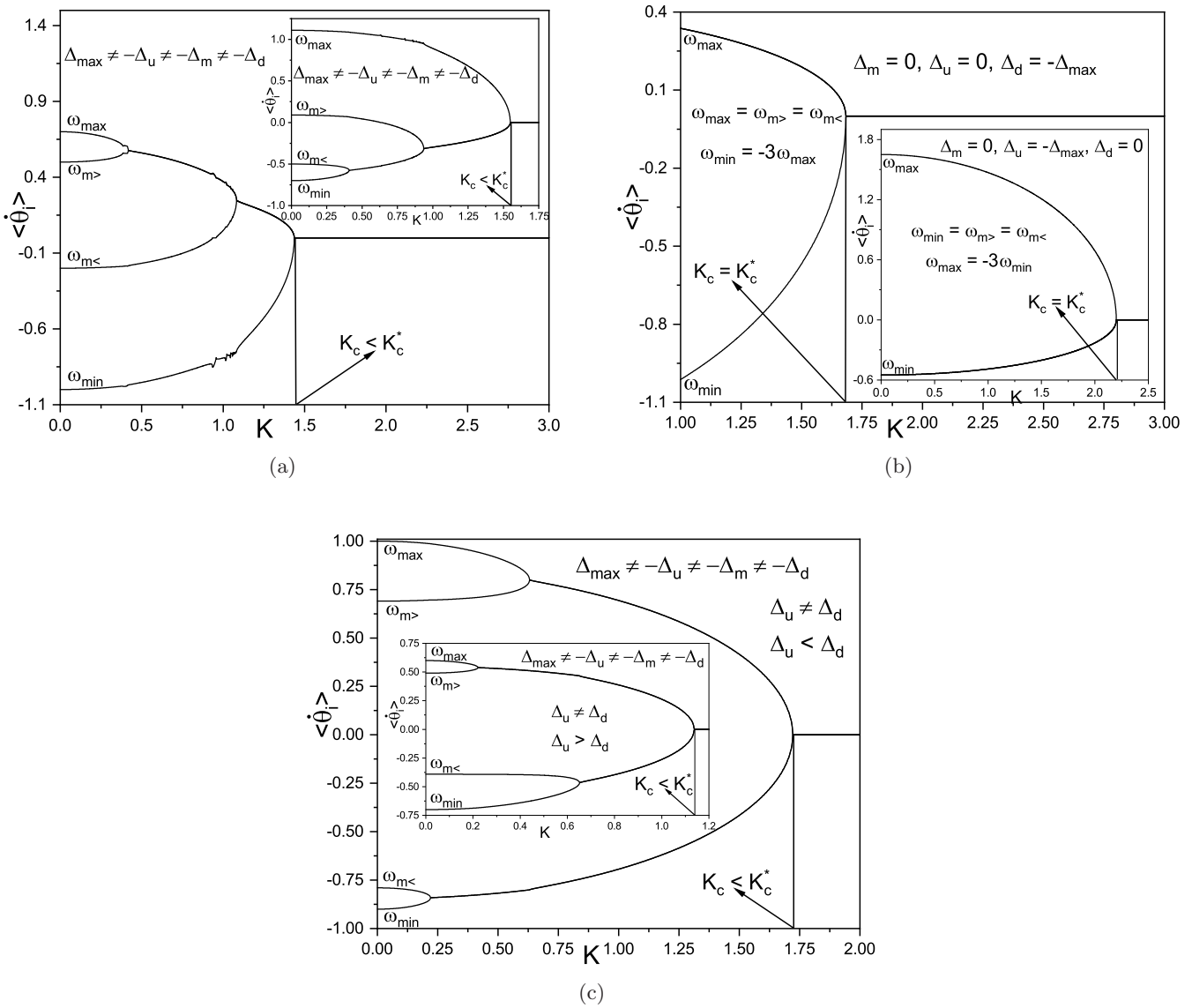

Fig. 1. Plots of $\langle \dot{\theta}_i \rangle$ versus K for six different patterns in the diagrams (a)–(c) and their insets. The different conditions of the initial frequencies and the frequency differences are indicated in each graph and its inset. Only the two cases in the plot (b) and its inset possess $K_c = K_c^*$. The other two plots (a) and (c) and their insets have $K_c < K_c^*$.

approaching from below ($\omega_{m<}$ and $\omega_{\min}$ of a larger separation). In all graphs of Figs. 1(a) and 1(c), and their insets, we show the values of the minimum couplings K_c and K_c^* that represent the occurrence of the partial phase locking and the full phase locking, where $K_c < K_c^*$, correspondingly. In the plots of Fig. 1(b), we demonstrate the case when $K_c = K_c^*$. In Fig. 2, we show other six cases of different configurations of the initial frequencies of the four oscillators, where the four different quantities $\langle \dot{\theta}_{\max} \rangle \simeq \langle \dot{\theta}_{m>} \rangle \simeq \langle \dot{\theta}_{m<} \rangle \simeq \langle \dot{\theta}_{\min} \rangle$ at K_c (the beginning of the partial phase locking). We show, in the legends of all plots of Fig. 2, the conditions for each pattern. Figure 2(a) demonstrates the case of the synchronization of oscillators that have initial frequencies of $\omega_{\max} = \omega_{m>}$ and $\omega_{m<} = \omega_{\min}$, where $\omega_{\max} = -\omega_{\min}$ and $\omega_{m>} = -\omega_{m<}$. The inset of Fig. 2(a) shows the case where the four oscillators meet at K_c once the initial frequencies are $\omega_{\max} = -\omega_{\min}$, $\omega_{m>} = -\omega_{m<}$, $\omega_{\max} \neq \omega_{m>}$ and $\omega_{m<} \neq \omega_{\min}$. In the plot in Fig. 2(b), we show the case when the two inner oscillators have closer initial frequencies $\omega_{m>} = -\omega_{m<}$ and the outer two oscillators have initial frequencies $\omega_{\max} = -\omega_{\min}$. Figure 2(c) shows the synchronization of the four oscillators that have $\omega_{\max} = -\omega_{\min}$ and $\omega_{m>} = \omega_{m<} \equiv \omega_o$. In the main graph of Fig. 2(a), we present the case when $K_c = K_c^*$, where K_c and K_c^*

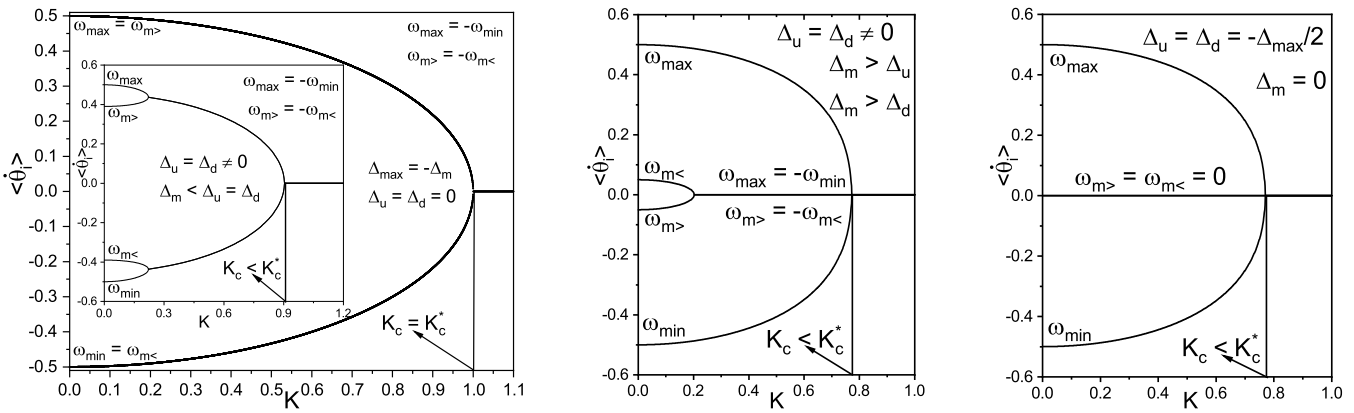

(a) (b) (c)

Fig. 2. (a)–(c) Three different graphs of $\langle\dot{\theta}_i\rangle$ against K for four different patterns. In the diagrams we show the initial frequencies and the frequency differences of each plot. The cases which are shown in the main plot of (a) shows $K_c = K_c^*$ while the other graphs show $K_c < K_c^*$.

represent the occurrence of the partial phase locking and the full phase locking, respectively. In the inset of Fig. 2(a) and the diagrams of Figs. 1(a) and 1(c), we show the values of the coupling constants $K_c < K_c^*$.

In all plots of Figs. 1 and 2, and their insets, we indicate K_c in the graphs, where the oscillators start to partially synchronize to each other, all still with $\dot{\theta}_j$, for $j = 1, 2, 3, 4$, as time dependent quantities. The four quantities $\langle\dot{\theta}_j\rangle$ possess numerical values within the order $[10^{-3} : 10^{-6}]$. The numerical values of K_c are measured assuring that the oscillators are in a partial locking state [Aeyels & Rogge, 2004; Mirollo & Strogatz, 2005; Chopra & Spong, 2009]. In particular, the average time evolution of the frequencies $< \dot{\theta}_j \sim 10^{-3}$ for the case is shown in Fig. 2(c). The values of the four quantities $\langle\dot{\theta}_j\rangle$ are less than 10^{-3}, as we go from the case in Fig. 2(c) to the cases in the plots of Fig. 2(b) and the inset of Fig. 2(a), and as we go from Fig. 2(c) to Figs. 1(a) and 1(c) as well as the plots in their insets. The values of $\langle\dot{\theta}_j\rangle$ become $\sim 10^{-6}$ when we have the cases as shown in Fig. 1(b) and the main plot of Fig. 2(a).

3. Oscillators at a Full Stable Phase Locking

We write explicitly Eq. (1), for four all-to-all coupled phase oscillators whenever the frequency synchronization occurs at a full phase locking, as

$$\begin{aligned}\dot{\theta}_{\max} &= \omega_{\max} + \frac{K_c^*}{4}[\sin^*(\theta_{m>} - \theta_{\max}) \\ &\quad + \sin^*(\theta_{m<} - \theta_{\max}) + \sin^*(\theta_{\min} - \theta_{\max})] \\ &= 0, \qquad (2a)\end{aligned}$$

$$\begin{aligned}\dot{\theta}_{m>} &= \omega_{m>} + \frac{K_c^*}{4}[\sin^*(\theta_{\max} - \theta_{m>}) \\ &\quad + \sin^*(\theta_{m<} - \theta_{m>}) + \sin^*(\theta_{\min} - \theta_{m>})] \\ &= 0, \qquad (2b)\end{aligned}$$

$$\begin{aligned}\dot{\theta}_{m<} &= \omega_{m<} + \frac{K_c^*}{4}[\sin^*(\theta_{\max} - \theta_{m<}) \\ &\quad + \sin^*(\theta_{m>} - \theta_{m<}) + \sin^*(\theta_{\min} - \theta_{m<})] \\ &= 0, \qquad (2c)\end{aligned}$$

and

$$\begin{aligned}\dot{\theta}_{\min} &= \omega_{\min} + \frac{K_c^*}{4}[\sin^*(\theta_{\max} - \theta_{\min}) \\ &\quad + \sin^*(\theta_{m>} - \theta_{\min}) + \sin^*(\theta_{m<} - \theta_{\min})] \\ &= 0. \qquad (2d)\end{aligned}$$

We take into consideration that the condition $\sum_{i=1}^{3}\omega_i = 0$ is maintained. We label the four frequencies, as mentioned earlier, $\omega_{\max} > \omega_{m>} > \omega_{m<} > \omega_{\min}$. Thus, the initial frequencies are $\{\omega_{\max} > \omega_{m>} > \omega_{m<} > \omega_{\min}\}$, where $\omega_{\max}$ and $\omega_{\min}$ are the maximum and the minimum initial

frequencies, correspondingly, while $\omega_{m>}$ and $\omega_{m<}$ are the two oscillators having initial frequencies in between the maximum and the minimum frequencies. The coupling strength K_c^* is the minimum value of the coupling constant at which the system is in a synchronized state having a stable phase locking solution. The four phases are $\theta_{\max}$, $\theta_{m>}$, $\theta_{m<}$ and $\theta_{\min}$. All the quantities θ_j and $\dot{\theta}_j$, for $j = 1, 2, 3, 4$, become time independent at K_c^* [Strogatz, 2018].

In order to examine the numerical findings searching for the parameters that control K_c^*, we study the numerical solutions of Eqs. (2) by using values of frequencies in different ranges of the set $\{\omega_{\max}, \omega_{m>}, \omega_{m<}, \omega_{\min}\}$. We are able to calculate numerically the synchronization coupling constant, $K_c^{*\mathrm{Num}}$, by integrating system (2) in several ranges of the maximum detuning $\Delta_{\max}$. We determine numerically $K_c^{*\mathrm{Num}}$ when $\langle(\dot{\theta}_j(t) - \dot{\theta}_i(t))\rangle \equiv (\dot{\theta}_j(t) - \dot{\theta}_i(t)) \equiv (\dot{\theta}_j - \dot{\theta}_i)$ become time independent and they possess numerical values of the order 10^{-6}. The numerical values of $K_c^{*\mathrm{Num}}$ are determined ensuring that the oscillators are in a stable fully phase locking [Aeyels & Rogge, 2004; Mirollo & Strogatz, 2005].

In order to represent how $K_c^{*\mathrm{Num}}$ depends on the frequency differences $\Delta_{\max} > 0$ and $\Delta_m < 0$, we determine numerically $K_c^{*\mathrm{Num}}/(\Delta_{\max} + 0.99\Delta_m)$ and $\Delta_{\max}/(\Delta_{\max} + 0.99\Delta_m)$, where the factor 0.99 exists in front of Δ_m to avoid any divergence when the frequency difference quantity Δ_m comes close to $-\Delta_{\max}$. We plot, in the main graph of Fig. 3, the computed values $K_c^*/(\Delta_{\max} + 0.99\Delta_m)$ versus $\Delta_{\max}/(\Delta_{\max} + 0.99\Delta_m)$. As a result, we show, in the main plot of Fig. 3, the transition into the synchronized states at a total stable phase locking in terms of the two parameters $\Delta_{\max}$ and Δ_m. The open circles in Fig. 3 denote the calculated values of $K_c^{*\mathrm{Num}}$, by integrating numerically system (2), in different ranges of $\{\omega_{\max}, \omega_{m>}, \omega_{m<}, \omega_{\min}\}$. The solid line represents Eq. (3) that shows a good matching with the numerical data. According to the findings in the main plot of Fig. 3, we obtain an approximate expression, for the coupling strength K_c^*, to be given as

$$K_c^{*\mathrm{app.}} \approx \Delta_{\max} + (\Delta_{\max} + 0.99\Delta_m) - \epsilon_o,$$

where

$$\epsilon_o = 1.185(\Delta_{\max} + 0.99\Delta_m), \qquad (3)$$

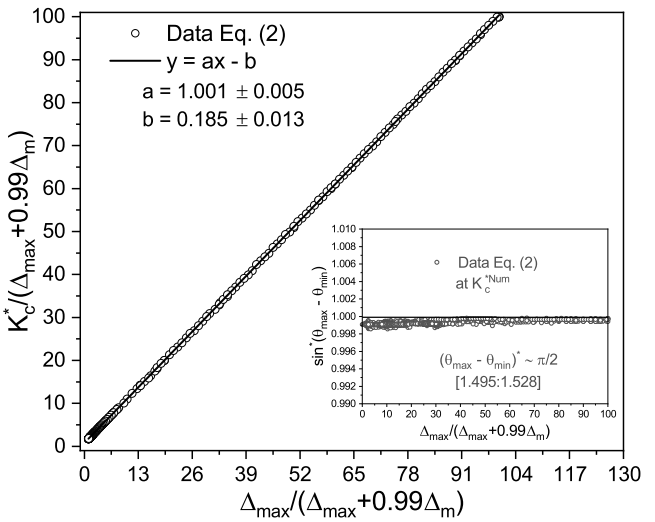

Fig. 3. The main plot displays the transition to the synchronous state at the complete stable phase locking. It also shows the accuracy of the parameters that lead to Eq. (3). The inset diagram indicates the phase lock condition at the transition to synchronization.

where the fitting parameters are indicated in the main diagram of Fig. 3. Then, we test the validity of the numerical approach that leads to relation (3), we obtain an error $(K_c^{*\mathrm{app.}} - K_c^{*\mathrm{Num}}) \leq \pm 10^{-1}$, where $K_c^{*\mathrm{Num}}$ is the critical value of coupling computed by numerically integrating Eq. (2) and $K_c^{*\mathrm{app.}}$ is the coupling at a fully phase locking which is calculated by using Eq. (3). It should be noted that we used several combinations other than $(\Delta_{\max} + 0.99\Delta_m)$ and $\Delta_{\max}/(\Delta_{\max} + 0.99\Delta_m)$ but these are the only combinations of the two parameters $\Delta_{\max}$ and Δ_m (as shown in Fig. 3) which allow us to obtain Eq. (3) with an error $(K_c^{*\mathrm{app.}} - K_c^{\mathrm{Num}}) \leq \pm 10^{-1}$. Therefore, the numerical findings allow us to suggest that the exact critical coupling should take the form

$$K_c^* = \Delta_{\max} + (\Delta_{\max} + 0.99\Delta_m) - \xi, \qquad (4)$$

where ξ is an unknown factor. Equation (4) shows that the coupling factor K_c^* depends on the frequency difference $\Delta_{\max} = (\omega_{\max} - \omega_{\min})$ [Chopra & Spong, 2009] as well as the frequency difference $\Delta_m = (\omega_{m<} - \omega_{m>})$, in addition to an indeterminate amount ξ. In order to have an exact expression of K_c^*, the quantity ξ must be determined exactly and it has to depend on both $\Delta_{\max}$ and Δ_m, in a different way than the term ϵ_o [as shown in Eq. (3)] and/or ξ must depend on other additional parameter(s) other than both $\Delta_{\max}$ and Δ_m.

We calculate the phase differences at $K_c^{*\mathrm{Num}}$ as presented in Eq. (2), where the state of full phase locking is assured and the stability conditions [Aeyels & Rogge, 2004; Mirollo & Strogatz, 2005] are fulfilled. We always find that $(\theta_{\max} - \theta_{\min})^* \sim \pi/2$, and principally $(\theta_{\max} - \theta_{\min})^*$ is in the interval $[1.527 : 1.551]$, where $(\dot{\theta}_{\max} - \dot{\theta}_{\min})$ is of the order of 10^{-6}. In this situation, we find $\sin(\theta_{\max} - \theta_{\min})^*$ is in the interval $[0.999 : 0.9997]$, for all values of initial frequencies and in different ranges of $\{\omega_{\max}, \omega_{m>}, \omega_{m<}, \omega_{\min}\}$; i.e. different widths $[\omega_{\min} : \omega_{\max}]$. We demonstrate the behavior of $(\theta_{\max} - \theta_{\min})^*$ at the inset plot of Fig. 3 at the complete frequency synchronization, when we plot $\sin^*(\theta_{\max} - \theta_{\min})$ versus $\Delta_{\max}/(\Delta_{\max} + 0.99\Delta_m)$. According to the results in the inset diagram of Fig. 3 at K_c^*, we are able to define the phase lock condition, as it directly comes from the results in the inset of Fig. 3. This phase lock condition is

$$(\theta_{\max} - \theta_{\min})^* \cong \frac{\pi}{2}, \tag{5}$$

which corresponds to the quantity $\Delta_{\max} = (\omega_{\max} - \omega_{\min}) > 0$ at the moment the oscillators transit to synchronization when the full phase locking is maintained.

Equations (3) and (4) indicate that the quantities $\Delta_{\max}$ and Δ_m control the value of K_c^*. For the best approximation, we can consider $\sin^*(\theta_{\max} - \theta_{\min}) = 1$. Thus, we depend on Eq. (2) to rewrite the difference equations of $\Delta_{\max}$ and Δ_m, when the condition (5) is satisfied. The four relations in Eq. (2) allow us to write the following relations,

$$\begin{aligned}\frac{4\Delta_{\max}}{K_c^*} &+ \sin^*(\theta_{m>} - \theta_{\max}) \\ &+ \sin^*(\theta_{m<} - \theta_{\max}) - \sin^*(\theta_{m>} - \theta_{\min}) \\ &- \sin^*(\theta_{m<} - \theta_{\min}) - 2 \cong 0\end{aligned} \tag{6a}$$

and

$$\begin{aligned}\frac{4\Delta_m}{K_c^*} &+ \sin^*(\theta_{\max} - \theta_{m<}) \\ &+ 2\sin^*(\theta_{m>} - \theta_{m<}) + \sin^*(\theta_{\min} - \theta_{m<}) \\ &- \sin^*(\theta_{\max} - \theta_{m>}) - \sin^*(\theta_{\min} - \theta_{m>}) \cong 0.\end{aligned} \tag{6b}$$

It should be pointed out that further improving of Eq. (3) can be achieved to get closer values of K_c^* to the values $K_c^{*\mathrm{Num}}$ but in terms of $\Delta_{\max}$ and Δ_m in addition to other quantities $\Delta' s$. However, we go to analytic investigation taking the opportunity that the numerical findings guide us to use Eqs. (5) and the equations containing $\Delta_{\max}$, Δ_m, $\omega_{\max}$, $\omega_{\min}$, $\omega_{m>}$ and $\omega_{m<}$. This is because the system of four all-to-all coupled phase oscillators contains six quantities of phase differences that allow to apply trigonometric relations and identities in order to do analytic work at K_c^*.

4. Analytic Solution at a Full Stable Phase Locking

Based on the outcomes of Eqs. (3)–(6), we have to use Eqs. (2) and the phase lock condition (5), in order to obtain an analytic formula for the coupling constant at the occurrence of complete frequency synchronization when the stable phase locking solution is provided. Specifically, first we focus on Eqs. (2a), (2b) and (6a) which include the quantities $\omega_{\max}$ and $\omega_{\min}$ and $\Delta_{\max}$. Second, we use relations (2b), (2c) and (6b) which incorporate $\omega_{m>}$, $\omega_{m<}$ and Δ_m. These two steps are necessary to find a mathematical equation which can be solved leading to an analytic expression for the coupling value K_c^*. Therefore, at the instant of a complete frequency synchronization when a total phase locking is satisfied, we rewrite Eqs. (2a) and (2b) as

$$\sin^*(\theta_{m>} - \theta_{\max}) + \sin^*(\theta_{m<} - \theta_{\max}) = 1 - \frac{4\omega_{\max}}{K_c^*}$$

and

$$\sin^*(\theta_{m>} - \theta_{\min}) + \sin^*(\theta_{m<} - \theta_{\min}) = \frac{4\omega_{\min}}{K_c^*} + 1,$$

where we employ the phase lock condition $(\theta_{\max} - \theta_{\min})^* \cong \pi/2$ and hence for the best approximation $\sin^*(\theta_{\max} - \theta_{\min}) = 1$. Squaring both equations above and adding them, taking into consideration Eq. (6a), we obtain

$$\begin{aligned}&\cos^*(\theta_{m<} - \theta_{m>}) \\ &\quad = \frac{-4K_c^*\Delta_{\max} + 8(\omega_{\max}^2 + \omega_{\min}^2)}{K_c^{*2}}.\end{aligned} \tag{7}$$

Then, at the moment the oscillators are in a full phase locking state, we use Eqs. (2b) and (2c) and writing them as

$$\begin{aligned}&\sin^*(\theta_{m>} - \theta_{\max}) + \cos^*(\theta_{m>} - \theta_{\max}) \\ &\quad = \sin^*(\theta_{m<} - \theta_{m>}) + \frac{4\omega_{m>}}{K_c^*}\end{aligned}$$

and

$$\sin^*(\theta_{\min} - \theta_{m<}) + \cos^*(\theta_{\min} - \theta_{m<}) = \sin^*(\theta_{m<} - \theta_{m>}) - \frac{4\omega_{m<}}{K_c^*}.$$

Squaring and taking the difference, concerning Eqs. (5) and (6), we obtain

$$\sin^*(\theta_{m<} - \theta_{m>}) = -\frac{\Delta_m(K_c^{*2} - 4K_c^*\Delta_{\max} + 8(\omega_{\max}^2 + \omega_{\min}^2))}{K_c(K_c^*\Delta_{\max} - 4(\omega_{\max}^2 + \omega_{\min}^2))}. \quad (8)$$

From both Eqs. (7) and (8), we arrive at the following fourth order polynomial

$$K_c^{*4}(\Delta_{\max}^2 - \Delta_m^2) + 4K_c^{*3}\Delta_{\max}(\Delta_m^2 + \Delta_{\max}^2 - 2(\omega_{\max}^2 + \omega_{\min}^2)) - 8(K_c^{*2}(\omega_{\max}^2 + \omega_{\min}^2)) \times (5\Delta_{\max}^2 + \Delta_m^2 - 2(\omega_{\max}^2 + \omega_{\min}^2)) + 128K_c^*\Delta_{\max}(\omega_{\max}^2 + \omega_{\min}^2)^2 - 128(\omega_{\max}^2 + \omega_{\min}^2)^3 = 0. \quad (9)$$

In view of the estimated Eq. (3) and the suggested Eq. (4), we can write the accepted solution of (9) to give the correct expression for K_c^* in terms of both $\Delta_{\max}$, Δ_m and ξ as

$$K_c^* = \Delta_{\max} + (\Delta_{\max} + 0.99\Delta_m) - \xi,$$

where

$$\xi = L - \frac{(M - \Delta_{\max}N + \sqrt{(P_1 + P_2)N})}{(\Delta_{\max}^2 - \Delta_m^2)},$$

$$L = 2\Delta_{\max} + 0.99\Delta_m,$$

$$M = \Delta_{\max}^3 - \Delta_{\max}(\Delta_m^2 - 4\omega_{\max}\omega_{\min}),$$

$$N = \sqrt{9\Delta_{\max}^4 + \Delta_m^4 - 10\Delta_m^2\Delta_{\max}^2 + 24\omega_{\max}\omega_{\min}(\Delta_{\max}^2 - \Delta_m^2) + 16\omega_{\max}^2\omega_{\min}^2},$$

$$P_1 = 6\Delta_{\max}^6 - 4\Delta_m^2\Delta_{\max}^4 - 2\Delta_m^4\Delta_{\max}^2 - 8\Delta_m^4\omega_{\max}\omega_{\min} + 8\Delta_{\max}^4\omega_{\max}\omega_{\min}$$

and

$$P_2 = 32\Delta_m^2\omega_{\max}^2\omega_{\min}^2 + 2(\Delta_{\max}^4 - \Delta_m^2\Delta_{\max}^2 - 4\Delta_m^2\omega_{\max}\omega_{\min}). \quad (10)$$

Equation (10) enables to calculate the exact values of the coupling factor K_c^* at the full phase locking. Additionally, in Eq. (10), the term ξ is given exactly, which shows a dependency on $\Delta_{\max}$, Δ_m in addition to quantities $\omega_{\max}$ and $\omega_{\min}$. Relation (10) also allows to draw a diagram, similar to the one displayed in Fig. 3, that demonstrates how the oscillators transit to complete synchronization at a stable full phase locked state for any set of initial frequencies $\{\omega_{\max}, \omega_{m>}, \omega_{m<}, \omega_{\min}\}$. Also, this Eq. (10) will permit to verify exactly the values of the coupling constant K_c^* in comparison to their numerically calculated data by integrating Eq. (2) resulting in a small error between the exact and the computed values of $K_c^{*\mathrm{Num}}$. Equation (10) shows that the coupling constant at the full phase lock is a function $K_c^* \equiv K_c^*(\Delta_{\max}, \Delta_{\min}, \omega_{\max}, \omega_{\min})$. However, before drawing a plot to validate formula (10), we must resolve the divergence problems that appears in computing the term ξ due to the presence of $1/(\Delta_{\max}^2 - \Delta_m^2)$. In particular, Eq. (10) experiences a computational divergence in the range $-0.996\Delta_{\max} > \Delta_m > -\Delta_{\max}$, where the term ξ is blown up. In order to overcome this divergence problem in the term ξ, we study the solution of (9) with Δ_m in the range $-0.996\Delta_{\max} > \Delta_m > -\Delta_{\max}$. As a consequence, the solution of (9), in this case, leads to a valid expression of K_c^* which takes the form

$$K_c^* = \Delta_{\max} + (\Delta_{\max} + 0.99\Delta_m) - \xi = \frac{2\Delta_{\max}}{1 + \sqrt{2 - \frac{\Delta_m^2}{\Delta_{\max}^2}}},$$

where

$$\xi = 2\Delta_{\max} + 0.99\Delta_m - \frac{2\Delta_{\max}}{1 + \sqrt{2 - \frac{\Delta_m^2}{\Delta_{\max}^2}}}. \quad (11)$$

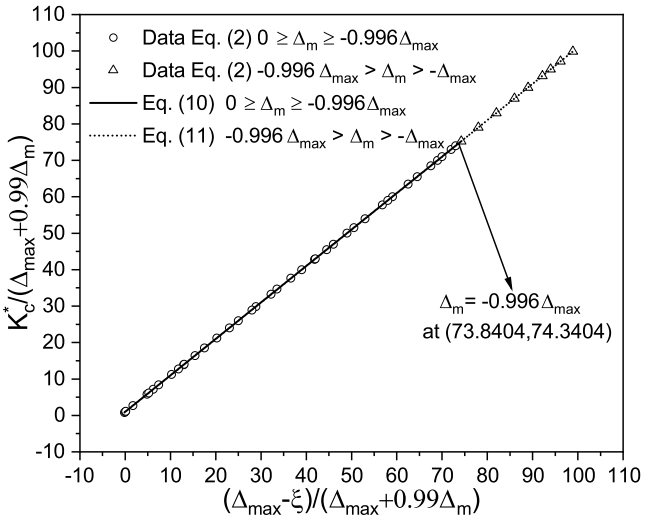

Fig. 4. The graph shows how the oscillators depart to the synchronization at a full phase locking depending on the frequency differences $\Delta_{\max}$ and Δ_m, in addition to the frequencies $\omega_{\max}$ and $\omega_{\min}$ according to Eqs. (10) and (11). The data computed numerically are shown in the plot. The ranges, where the relations (10) and (11) remain acceptable, are marked in the plot.

Therefore, we use Eq. (11) to calculate K_c^* as soon as we find a divergence of the term ξ upon using Eq. (10), which includes $1/(\Delta_{\max}^2 - \Delta_m^2)$, at a range $-0.996\Delta_{\max} > \Delta_m > -\Delta_{\max}$.

We use Eqs. (10) and (11) to draw the diagram as seen in Fig. 4 to illustrate the transition to a full phase locking state where oscillators are in synchronization, for any frequency differences $\Delta_{\max}$ and Δ_m as well as any frequencies $\omega_{\max}$ and $\omega_{\min}$. The diagram in Fig. 4 shows a plot of $K_c^*/(\Delta_{\max} + 0.99\Delta_m)$ versus $(\Delta_{\max} - \xi)/(\Delta_{\max} + 0.99\Delta_m)$. Equation (10) is computationally valid in the range $0 \geq \Delta_m \geq -0.966\Delta_{\max}$ (solid black line), while formula (11) is applicable when $-\Delta_{\max} < \Delta_m < -0.966\Delta_{\max}$ (black dotted-line). It is clearly indicated in Fig. 4 that we find a complete agreement between K_c^* (analytic) and $K_c^{*\mathrm{Num}}$ (calculated numerically). The numerical data, obtained by using Eq. (2) in the range $0 \geq \Delta_m \geq -0.966\Delta_{\max}$, is shown as circles while those points computed in the range $\Delta_{\max} < \Delta_m < -0.966\Delta_{\max}$ are plotted as triangles. Figure 4 displays the matching between the numerically calculated data (circles and triangles) and Eqs. (10) and (11), which are represented by the solid black line and the black dotted-line, respectively. We refer, in Fig. 4, to the point where the term ξ diverges at the (73.8404, 74.3404) coordinates. In Fig. 4, the zone above the solid lines represents the complete frequency synchronized states at a stable phase locking solution. Equations (10) and (11) together in the full range of $(\Delta_{\max} - \xi)/(\Delta_{\max} + 0.99\Delta_m)$ represent the border when the effective coupling passes ($K > K_c^*$), the oscillators go to a stable state of complete phase locking. When $K < K_c^*$ the system is in an unstable state of a partial phase locking [Aeyels & Rogge, 2004; Mirollo & Strogatz, 2005].

Expressions (10) and (11) explain the suitability of the numerical approach that leads to find Eqs. (3) and (4). However, formulas (10) and (11) allow to obtain exactly the term ξ that gives the correct K_c^* instead of the terms ϵ_o and the unknown factor ξ in Eqs. (3) and (4), respectively. Henceforward, relations (10) and (11) give the closest match between the analytically calculated K_c^* and the numerically computed $K_c^{*\mathrm{Num}}$. We find an error $|K_c^* - K_c^{*\mathrm{Num}}|$ is in a range $[5 \times 10^{-4} : 10^{-5}]$. This is because the system of four all-to-all coupled phase oscillators contains six phase differences that allows to apply trigonometric relations and identities in order to do analytic work at K_c^*.

5. Phase Differences at a Full Stable Phase Locking

At the moment the oscillators transit to a synchronous state, the phase lock condition $\sin^*(\theta_{\max} - \theta_{\min}) = 1$ takes place. Also, we know the correct expressions for K_c^*. Therefore, we can calculate all the phase differences at the moment the frequency synchronization occurs. Consequently, at the coupling value K_c^*, we have the following relations

$$\sin^*(\theta_{\max} - \theta_{\min}) \cong 1,$$

$$\sin^*(\theta_{m>} - \theta_{\max}) = \frac{K_c^* - 4\omega_{\max} - (K_c^* + 4\omega_{\min})\sqrt{\dfrac{K_c^{*2} + 4K_c\Delta_{\max} - 8(\Delta_{\max}^2 + 2\omega_{\max}\omega_{\min})}{K_c^{*2} - 4K_c^*\Delta_{\max} + 8(\Delta_{\max}^2 + 2\omega_{\max}\omega_{\min})}}}{2K_c^*},$$

$$\sin^*(\theta_{m<}-\theta_{m>})=-\frac{\Delta_m(K_c^{*2}-4K_c^*\Delta_{\max}+8(\Delta_{\max}^2+2\omega_{\max}\omega_{\min}))}{K_c^*(K_c^*\Delta_{\max}-4(\Delta_{\max}^2+2\omega_{\max}\omega_{\min}))},$$

$$\sin^*(\theta_{\min}-\theta_{m<})=\frac{K_c^*+4\omega_{\min}-(K_c^*-4\omega_{\max})\sqrt{\dfrac{K_c^{*2}+4K_c^*\Delta_{\max}-8(\Delta_{\max}^2+2\omega_{\max}\omega_{\min})}{K_c^{*2}-4K_c\Delta_{\max}+8(\Delta_{\max}^2+2\omega_{\max}\omega_{\min})}}}{2K_c^*},$$

$$\sin^*(\theta_{m<}-\theta_{\max})=\frac{K_c^*-4\omega_{\max}+(K_c^*+4\omega_{\min})\sqrt{\dfrac{K_c^2+4K_c\Delta_{\max}-8(\Delta_{\max}^2+2\omega_{\max}\omega_{\min})}{K_c^{*2}-4K_c^*\Delta_{\max}+8(\Delta_{\max}^2+2\omega_{\max}\omega_{\min})}}}{2K_c^*}$$

and

$$\sin^*(\theta_{\min}-\theta_{m>})=\frac{K_c^*+4\omega_{\min}+(K_c^*-4\omega_{\max})\sqrt{\dfrac{K_c^{*2}+4K_c^*\Delta_{\max}-8(\Delta_{\max}^2+2\omega_{\max}\omega_{\min})}{K_c^{*2}-4K_c^*\Delta_{\max}+8(\Delta_{\max}^2+2\omega_{\max}\omega_{\min})}}}{2K_c^*},\tag{12}$$

which can be used to calculate the phase differences at the effective coupling K_c^*. Particularly, in order to use the relations in (12), we substitute K_c^* by either employing the relation (10) in the range $0 \geq \Delta_m > -0.966\Delta_{\max}$ or we use formula (11) instead, which is applicable in the range $-\Delta_{\max} < \Delta_m < -0.966\Delta_{\max}$.

6. Discussion

Equations (10) and (11) characterize the edge between the stable state of complete phase locking and the unstable partial phase locking state. Expressions (10) and (11) give the values of the coupling factor K_c^*, for four nonidentical oscillators, in the neighborhood of, but less than, $\Delta_{\max}$ ($K_c^* \sim \Delta_{\max}$) for three cases where some oscillators have closed values of initial frequencies. The first case results when the oscillators have values of initial frequencies $\omega_{\max} \sim -\omega_{\min}$, $\omega_{m>} \lesssim \omega_{\max}$ and $\omega_{m<} \gtrsim \omega_{\min}$, where $\Delta_m \lesssim -\Delta_{\max}$. The second case happens as $\Delta_m \sim 0$ and when the conditions $\omega_{\max} \sim -3\omega_{\min}$ and $\omega_{m>} \sim \omega_{m<} \sim \omega_{\min}$ are maintained. The third case occurs when conditions $\omega_{\min} \sim -3\omega_{\max}$ and $\omega_{m>} \sim \omega_{m<} \sim \omega_{\min}$ are preserved and $\Delta_m \sim 0$. All previous three cases have features of initial frequencies which are far from being equal to the common frequency value which the oscillators possess at synchronization. Additionally, there is a final case, where Eqs. (10) and (11) provide values for the coupling strength K_c^* which approaches $2\Delta_{\max}/(1+\sqrt{2}) \sim 0.8285\Delta_{\max}$ when the oscillators have the conditions Δ_m close to zero, $\omega_{\max} \sim -\omega_{\min}$ and $\omega_{m>} \sim -\omega_{m<} \sim 0$. This last case is characterized by two initial frequencies being far from the common frequency and two initial frequencies very close to it.

These proceeding observations suggest that a further study is needed for the situations of coupled phase oscillators when the previously mentioned cases are noticed. Also, further studies are required to investigate the special cases when some oscillators have equal initial frequencies. Particularly, the studies must show how the three cases of initial frequencies far from the common frequency value are different in comparison to the case of two initial frequencies being close to the common frequency value. They also must show how the oscillators are approaching synchronization in the cases: (1) $\omega_{\max} = -\omega_{\min}$, $\omega_{m>} = \omega_{\max}$, $\omega_{m<} = \omega_{\min}$ and $\Delta_m = -\Delta_{\max}$. (2) $\Delta_m = 0$, $\omega_{\max} = -3\omega_{\min}$ and $\omega_{m>} = \omega_{m<} = \omega_{\min}$. (3) $\Delta_m = 0$, $\omega_{\min} = -3\omega_{\max}$ and $\omega_{m>} = \omega_{m<} = \omega_{\min}$. (4) $\Delta_m = 0$, $\omega_{\max} = -\omega_{\min}$ and $\omega_{m>} = -\omega_{m<}$ and, $\omega_{m>}$ and $\omega_{m<}$ are starting to be close to zero or $\omega_{m>} = \omega_{m<} = 0$.

Additional examinations have to be conducted in general not only at K_c^* but also at $K_c^* \geq K \geq K_c$ in order to analyze how the oscillators arrive at synchronization either at the incomplete phase lock states or at the fully phase locking. The numerical examinations of system (2) indicate clearly the starting of synchronization at the critical coupling K_c, which is close to the same as K_c^* when the oscillators' initial frequencies are far from the common frequency value. On the other hand, the numerical

investigations of system (2) at critical coupling, when some initial frequencies are close to the common frequency value, show that $K_c < K_c^*$. The difference between K_c and K_c^* starts to increase as middle frequencies become closer to the common frequency. The maximum difference between K_c and K_c^* approaches 0.059 in the case of conditions Δ_m close to zero, $\omega_{\max} \sim -\omega_{\min}$ and $\omega_{m>} \sim -\omega_{m<}$. The availability of the expressions (10) and (11) valid for calculating K_c^* will help to obtain a formula for calculating the values of the critical coupling K_c, where synchronization starts. Also, the detailed stability analysis have to be carried out for all values of $K_c^* \geq K \geq K_c$ and in different ranges of $\Delta_{\max}$ for different sets of $\{\omega_{\max}, \omega_{m>}, \omega_{m<}, \omega_{\min}\}$ including the special cases of some frequencies being equal.

The study of the individual oscillators at K_c^* and K_c, considering their phase differences, will help to recognize the dynamics when the oscillators start to fall into synchronization. This study has to be carried out knowing relations (12) that allow examining the phase differences at K_c^* and comparing these examinations with the numerical results of the phase differences at K_c. This will help to understand more about the difference between the complete phase locking and partially phase locking states for the four coupled all-to-all oscillators, especially when the difference between K_c^* and K_c starts to be noticeable. Also, the analysis of the phase shifts between phase differences at K_c^* and that at K_c will help to grasp synchronization procedures. Furthermore, in future works we will explore further recognition of the behavior of the four-coupled phase oscillators and we will obtain an expression for K_c.

7. Conclusion

We have studied a system of four globally coupled phase oscillators within the Kuramoto model at the transition to synchronization for a fully phase locking. The numerical study helps to distinguish the main frequency differences that rule the coupling strength K_c^*. Also, the numerical calculations help to obtain the approximate expression (3) which allows us to calculate the values of K_c^* that have a small fluctuation around the accurate value of the coupling factor at the complete phase locked states. Then we are able to identify the phase lock condition, where the phase difference $(\theta_{\max} - \theta_{\min})^* \sim \pi/2$ at the full phase locking state corresponds to the maximum frequency difference $\Delta_{\max}$. This phase lock condition allows us to use the proper equations to express the time evolution of phases and the time evolutions of the phase differences to obtain a fourth order polynomial of the critical coupling. Therefore, we are able to find a valid solution, for the given fourth order polynomial (9), to obtain mathematical expressions for the effective coupling K_c where the correct expressions (10) and (11), for the coupling constant at a full phase locking, show dependencies on the initial frequencies of the four oscillators. In Eq. (12) we obtain explicit relations for the phase differences, when the phase lock condition occurs at the transition to a stable phase locking.

The results found here will help to obtain solutions, at synchronous states, for a small number of globally coupled phase oscillators, where the number of oscillators is too small to use mean field calculations. Having more understanding of the dynamics of a few coupled phase oscillators will help to realize synchronization mechanisms, at the full phase lock states, for a finite, but small, number of oscillators. Thus, for a small number of globally coupled oscillators, the numerical approach that leads to Eq. (3) can be used to estimate solutions in cases where we encounter difficulties to obtain an analytic solution. The numerical computations and simulations in this case facilitate obtaining solutions because the number of phase difference quantities increases rapidly as the number of oscillators increases. This will introduce difficulties in utilizing trigonometric identities in order to have analytic solutions. Also, the numerical work will help in the study of phase differences as well as the shifts between the phase differences that may lead to relations that link some phase differences to some quantities of frequency differences. Thus, the determination of the coupling factor for four all-to-all Kuramoto oscillators at a full phase locking will help to obtain a formula for the critical coupling K_c at which the oscillators start to synchronize but having an unstable phase lock. Furthermore, the realization of stable synchronization procedures of four-coupled oscillators will help, in case of a few oscillators, to understand how these oscillators fall into synchronous states when they have initial frequencies far from or close to the mean frequency value. Moreover, being familiar with the mechanisms of synchronization, at a complete phase lock, of four-coupled

phase oscillators will help to realize the synchronization features and stability investigations for a larger number than four not only for the globally coupled systems of oscillators but also for systems of nearest neighbors coupled oscillators in a ring either in cases of bidirectional coupling or in situations of unidirectional coupling. The frequency synchronization mechanisms for a limited number of oscillators, might strengthen the construction of systems which function in various applications [Kreinberg *et al.*, 2019; DeTal *et al.*, 2019; Blanter & Shnirman, 2020; Frolov *et al.*, 2020].

Acknowledgment

H. A. Cerdeira thanks ICTP-SAIFR and FAPESP Grant 2016/01343-7 for partial support.

References

Aeyels, D. & Rogge, J. A. [2004] "Existence of partial entrainment and stability of phase locking behavior of coupled oscillators," *Progr. Theoret. Phys.* **112**, 921–942.

Blanter, E. & Shnirman, M. [2020] "Inverse problem in the Kuramoto model with a phase lag: Application to the sun," *Int. J. Bifurcation and Chaos* **30**, 2050165-1–15.

Boccaletti, S., Pisarchik, A. N., Del Genio, C. I. & Amann, A. [2018] *Synchronization*: *From Coupled Systems to Complex Networks* (Cambridge Univ. Press., Cambridge, UK).

Chhea, K., Ron, D. & Lee J.-R. [2020] "Application of Kuramoto model to transmission power control in wireless body area networks," *IEEE Access* **8**, 213531–213540.

Chopra, N. & Spong, M. W. [2009] "On exponential synchronization of Kuramoto oscillators," *IEEE Trans. Autom. Contr.* **54**, 353–357.

Csaba, G. & Porod, W. [2020] "Coupled oscillators for computing: A review and perspective," *Appl. Phys. Rev.* **7**, 011302-1–19.

DeTal, N., Taheri, H. & Wiesenfeld, K. [2019] "Synchronization behavior in a ternary phase model," *Chaos* **29**, 063115-1–7.

El-Nashar, H. F. [2016] "Exact solution at a transition to frequency synchronization of three coupled phase oscillators," *Can. J. Phys.* **94**, 808–813.

El-Nashar, H. F. [2017] "Conditions and linear stability analysis at the transition to synchronization of three coupled phase oscillators in a ring," *Int. J. Bifurcation and Chaos* **27**, 1750095-1–15.

Fernández, S. L. & Porras, D. [2021] "Dissipative Josephson effect in coupled nanolasers," *New J. Phys.* **23**, 033010-1–21.

Frolov, N., Maksimenko, V. & Ghosh, D. [2020] "Route to coherence in a frequency-heterogeneous Kuramoto network," *Fourth Scientific School on Dynamics of Complex Networks and Their Application in Intellectual Robotics* (*DCNAIR*) (Innopolis, Russia), pp. 82–84.

Gourary, M. M. & Rusakov, S. G. [2020] "Kuramoto model for oscillators with fractional frequencies ratios in circuit analysis application," *IEEE East–West Design and Test Symp.* (*EWDTS*) (Varna, Bulgaria), pp. 88–91.

Guo, Y., Zhang, D., Li, Z., Wang, Q. & Yu, D. [2021] "Overviews on the applications of the Kuramoto model in modern power system analysis," *Electr. Pow. Energ. Syst.* **129**, 106804-1–11.

Heggli, O. A., Cabral, J., Konvalinka, I., Vuust, P. & Kringelbach, M. L. [2019] "A Kuramoto model of self-other integration across interpersonal synchronization strategies," *PLOS Comput. Biol.* **16**, 1–17.

Huang, K. & Zadeh, M. H. [2020] "Detection and sensing using coupled oscillatory systems at the synchronization edge," *IEEE Sensors J.* **20**, 12992–12998.

Jang, J. K., Ji, X., Joshi, C., Okawachi, Y., Lipson, M. & Gaeta, A. L. [2019] "Observation of Arnold tongues in coupled soliton Kerr frequency combs," *Phys. Rev. Lett.* **123**, 153901-1–7.

Kreinberg, S., Porte, X., Schicke, D., Lingnau, B., Schneider, C., Höfling, S., Kanter, I., Lüdge, K. & Reitzenstein, S. [2019] "Mutual coupling and synchronization of optically coupled quantum-dot micropillar lasers at ultra-low light levels," *Nature Commun.* **10**, 1539-1–11.

Latifpour, M. H. & Miri, M. A. [2020] "Mapping the XY Hamiltonian onto a network of coupled lasers," *Phys. Rev. Res.* **2**, 043335-1–7.

Maistrenko, Yu., Popovych, O., Burylko, O. & Tass, P. A. [2004] "Mechanism of desynchronization in the finite-dimensional Kuramoto model," *Phys. Rev. Lett.* **93**, 084102-1–4.

Maistrenko, Yu., Burylko, O. & Tass, P. A. [2005] "Chaotic attractor in the Kuramoto model," *Int. J. Bifurcation and Chaos* **15**, 3457–3466.

Mirollo, R. E. & Strogatz, S. H. [2005] "The spectrum of the locked state for the Kuramoto model of coupled oscillators," *Physica D* **205**, 249–266.

Scholes, G. D. [2020] "Limits of exciton delocalization in molecular aggregates," *Farad. Discuss.* **221**, 143265–143280.

Strogatz, S. [2018] *Nonlinear Dynamics and Chaos with Applications to Physics*, *Biology*, *Chemistry*, *and Engineering*, 2nd edition (CRC Press, NY, USA).

Taheri, H., Del'Haye, P., Eftekhar, A. A., Wiesenfeld, K. & Adibi, A. [2017] "Self-synchronization phenomena in the Lugiato–Lefever equation," *Phys. Rev. A* **96**, 013828-1–9.

Thiem, T. N., Kooshkbaghi, M., Bertalan, T., Laing, C. R. & Kevrekidis, I. G. [2020] "Emergent spaces for coupled oscillators," *Front. Comput. Neurosci.* **14**, 36-1–19.

Velasco, V. & Neto, M. B. S. [2021] "Unconventional superconductivity as a quantum Kuramoto synchronization problem in random elasto-nuclear oscillator networks," *J. Phys. Commun.* **5**, 015003-1–14.

Wiesenfeld, K. [2020] "Synchronization in disordered superconducting arrays," *J. Phys. A*: *Math. Theor.* **53**, 064002-1–19.

Witthaut, D., Wimberger, S., Burioni, R. & Timme, M. [2017] "Classical synchronization indicates persistent entanglement in isolated quantum systems," *Nature Commun.* **8**, 14829-1–7.

Wu, J. & Li, X. [2020] "Collective synchronization of Kuramoto-oscillator networks," *IEEE Circuits Syst. Mag.* **20**, 46–67.

Yang, L. X. & Liu, X. J. [2020] "Nonlinear dynamics and control," *Proc. First Int. Nonlinear Dynamics Conf.* (NODYCON 2019), pp. 295–303.

Yap, R. M. S., Ogawa, K., Hirobe, Y., Nagashima, T., Seki, M., Nakayama, M., Ichiryu, K. & Miyake, Y. [2019] "Gait-assist wearable robot using interactive rhythmic stimulation to the upper limbs," *Front. Robot. AI* **6:25**, 1–11.

Young-Pil, C. & Zhuchun, L. [2019] "Synchronization of nonuniform Kuramoto oscillators for power grids with general connectivity and dampings," *Nonlinearity* **32**, 559–583.